

## Brief Note

# Spatial Gradient Interface Detection in Topology Optimization for an Unstructured Mesh

Luke Crispo<sup>1</sup>, Rubens Bohrer<sup>1</sup>, Stephen W. K. Roper<sup>1</sup>, Il Yong Kim<sup>1</sup>

<sup>1</sup>Department of Mechanical and Materials Engineering, Queen's University, 130 Stuart St. Kingston, Ontario, K7L 3N6, Canada

### Abstract

Spatial gradient calculations are regularly applied in topology optimization and typically used for detecting material distribution boundaries, interfaces, and overhanging features. While adopted for a variety of applications, the current approaches in literature are restricted to perfectly uniform mapped-meshing strategies or require element shape function vectors to complete computations, both of which are potential limitations when solving practical problems with commercial finite element solvers. To address these drawbacks, this brief note presents a technique for calculating spatial gradients using a neighbouring element search strategy, using the gradient norm, thinning, and thresholding calculations to determine a nearly discrete interface indicator. The proposed technique is generalized for a 3D unstructured mesh and applicable when using black-box finite element solvers. The technique is validated on three sample problems with increasing geometric and mesh discretization complexity to demonstrate and suggest its effectiveness for topology optimization in 2D and 3D.

**Keywords** Interface Detection, Spatial Gradient, Topology optimization

### 1 Introduction

The spatial gradient calculation is used in a variety of topology optimization (TO) problems, with the norm of the spatial gradient used to detect boundaries within a pseudo-density field and the spatial gradient vector used to determine surface orientations. Interface detection was originally used as a perimeter control method to prevent checkerboarding (Zhou et al. 2001) but has more recently been employed in advanced TO approaches in the field of additive manufacturing for surface area calculations and support structure calculations (Ryan and Kim 2019, Sabiston and Kim 2019), and overhang angle calculations (Qian 2017). Boundary detection has also been found critical to multi-material and multi-joint topology optimization, where it is used to locate the regions between components and precisely update the model with more accurate joint properties (Woischwill and Kim 2018, Florea et al. 2020). Other interface detection applications in TO include: coated structures (Clausen et al. 2015) and adaptive mesh refinement (Stainko 2006, Nana et al. 2016) to name a few.

Generally, spatial gradient and interface detection techniques can be categorized into three approaches: (1) structured methods that rely on perfectly uniform finite element (FE) discretization, (2) nodal density methods that rely on shape function derivatives, and (3) neighbouring element methods. Structured approaches rely on the grid-like nature of a perfect quadrilateral FE

mesh and are typically seen in simple academic test problems. Here, spatial gradients are calculated based on the difference in element densities above/below and left/right of the element of interest (Stolpe and Svanberg 2001) or with Sobel gradient operators (Yang et al. 2019). The second technique relies on translating element-based pseudo-densities to nodal densities and calculates spatial gradients based on the derivative of the element shape function vector (Ryan and Kim 2019). Neighbouring element approaches rely on the difference in density between a central element and its neighbours to identify interfaces. If element pseudo-densities are thresholded to discrete 0-1 values, interfaces can be identified through a simple loop that searches for void elements that share edges with any other solid elements (Costa Jr and Alves 2003, Woischwill and Kim 2018). A proposed neighbouring element approach, that does not require element thresholding, calculates an aggregate difference in element density across all of a central element's edges (Beckers 1999). These approaches, also known as perimeter calculations, rely only on directly adjacent elements in interface calculations. Performing a calculation using a search radius around a central element, similar to standard TO density and sensitivity filtering, would improve performance in triangular and tetrahedral meshes, where an element may only share edges with a small number of its adjacent elements. A search radius allows for interface detection to be defined independently from element size and FE discretization.

## Brief Note

One proposed search radius method determines interfaces based on the difference between filtered element densities and the original design variables values (Stainko 2006). This method was applied to refine a FE mesh along element boundaries of converged TO results, but would be less effective on designs with many intermediate density elements as there would be little difference between the filtered and unfiltered densities.

While effective, methods (1) and (2) have limitations when solving TO problems featuring complex geometry or loading requiring use of commercial FE solvers. In these cases, structured approaches are inherently limited by pre-processing the complex geometry. Nodal density methods are limited in the solution process, with most commercial FE solvers limiting user access to the stiffness matrix and shape function vectors. Neighbouring element methods are the most promising as they can be easily implemented with commercial solvers by using the solver input files to obtain node and element information. However, performance is tied to element discretization in element edge approaches, and the quantity of intermediate density elements for the filtering approach by Stainko.

The objective of this work is to develop a search radius-based interface detection methodology that can be applied to unstructured 3D FE meshes and can interface with commercial solvers without relying on element shape function derivatives. This method does not rely on FE discretization and can be applied to problems with many intermediate density elements. The proposed technique will be validated on optimization problems to calculate a near-discrete interface indicator for unstructured 2D and 3D meshes.

## 2 Methodology

The spatial density gradient of the  $e$ -th finite element in the  $j$ -th direction,  $\nabla_j \rho_e$ , can be calculated using a modification of a common topology optimization density filter (Sigmund 2007), expressed as:

$$\nabla_j \rho_e = \frac{\sum_{k=1}^N H_k v_k \rho_k \cos \theta_{j,k}}{\sum_{k=1}^N H_k v_k} \quad (1)$$

$$H_k = \max \{0, r - \|\vec{u}_{e,k}\| \}$$

where  $H_k$  is a distance term with a maximum value equal to the filter radius  $r$ . This term decreases to 0 as the magnitude of the vector from the center of the  $e$ -th element to the  $k$ -th neighbouring element,  $\vec{u}_{e,k}$ , increases. The summation in the numerator of (1)

determines the gradient in the  $j$ -th direction by multiplying the element pseudo-density  $\rho_k$  by the cosine of the angle  $\theta_{j,k}$ , which is the angle between the unit vector  $\hat{e}_j$  in the  $j$ -th direction and the vector  $\vec{u}_{e,k}$ . A neighbouring element's influence on the spatial gradient is also weighted based on its size through multiplication of the element volume,  $v_k$ . The spatial gradient term is normalized by dividing by the summation of the distance and volume terms in the denominator. Both summations include the  $N$  neighbouring elements that fall within the search radius

This is depicted graphically in Fig. 1 for a uniform mesh where the spatial gradient of the central element is computed in the  $x$  and  $y$  direction. The cosine term will yield a positive value between 0 and 1 when the angle  $\theta_{j,k}$  is acute, which occurs when the  $k$ -th element is in the  $+j$  direction relative to the  $e$ -th element. The cosine term results in negative values for obtuse angles, when the  $k$ -th element is in the  $-j$  direction, and provides a value of 0 when  $\theta_{j,k}$  is a right angle. This yields positive or negative weighting factors for the surrounding elements to calculate the spatial gradient in the specified direction.

Spatial Gradient in  $x$  Direction ( $j=1$ )      Spatial Gradient in  $y$  Direction ( $j=2$ )

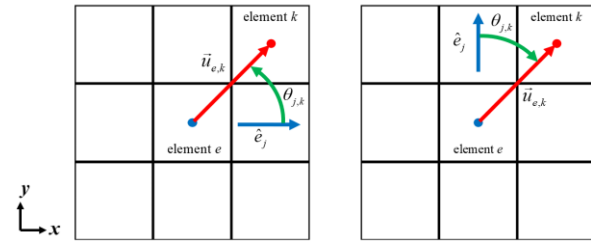


Fig. 1 Interface detection formulation applied in a 2D uniform grid outlining the contribution of the  $k$ -th element to the gradient of the  $e$ -th element in each direction.

A spatial gradient vector is formed from the components of the spatial gradient in each direction. This vector measures the orientation of the surface and can be used to detect overhangs within a geometry. To determine interfaces, the magnitude of the spatial gradient can be calculated as follows:

$$n_e = \|\nabla_j \rho_e\| = \sqrt{\sum_{j=1}^M (\nabla_j \rho_e)^2}, \quad j = 1, \dots, M \quad (2)$$

where  $n_e$  is the spatial gradient magnitude of the  $e$ -th element, and  $M$  is the number of spatial dimensions of the problem. The spatial gradient magnitude is a pseudo-interface term that identifies all boundaries of the geometry. This term can be manipulated in subsequent equations depending on the TO application. In this paper,

## Brief Note

two additional steps (thinning and Heaviside discretization) were performed. First, the thinned spatial gradient magnitude,  $\hat{n}_e$ , can be calculated using (3). Multiplying by  $(1-\rho_e)$  removes interface values in solid elements, resulting in only the elements surrounding the geometry being identified as an interface. This also has the effect of eliminating interfaces at the boundaries of the design space.

$$\hat{n}_e = (1 - \rho_e)n_e \quad (3)$$

A smooth Heaviside approximation can be used next to obtain more discrete interface values, which are desired in most TO approaches. The projected spatial gradient magnitude,  $\tilde{n}_e$ , can be calculated using the following equation:

$$\tilde{n}_e = \frac{1}{1 + e^{-2\beta(\hat{n}_e - \eta)}} \quad (4)$$

where  $\beta$  and  $\eta$  are parameters that adjust the slope and inflection point of the function, respectively.

### 3 Numerical examples

The proposed methodology was implemented in a custom Fortran code that interfaces with Altair's OptiStruct (Altair 2019) finite element input decks and was applied to three numerical examples to demonstrate its performance on models of varying mesh complexity. Each example uses element densities from topology optimization problems that are not pertinent to the interface detection. A search radius of twice the average mesh size was used for each example.

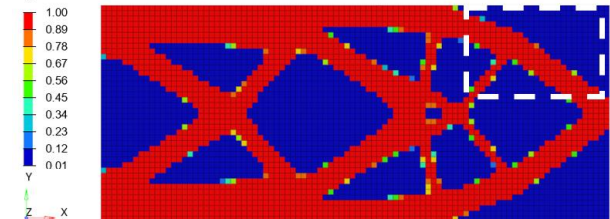
#### 3.1 Structured 2D mesh

The topology optimization element densities used for this example are displayed in Fig. 2a, showing a 2D structured quadrilateral mesh. Interface detection in this mesh can be accomplished in a variety of ways, many of which rely on the structured nature of the element layout. The spatial gradient of element density in the  $x$  and  $y$  directions is shown in Fig. 2b-c. The spatial gradient is positive or negative depending on whether element density is increasing or decreasing in the associated direction.

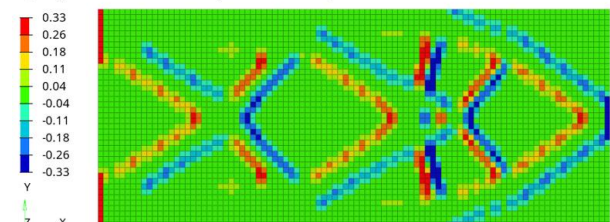
The remaining steps in the interface detection calculation are depicted in Fig. 3 for the boxed subsection of the geometry in Fig. 2a. First the magnitude of the spatial gradient calculates an interface value and removes any negative terms from the spatial gradients. Next the thinning calculation removes all interfaces that overlap with element densities, resulting in an interface that is a single layer thick that surrounds the geometry. Lastly, the

Heaviside projection produces a nearly discrete interface, where parameters  $\beta$  and  $\eta$  were defined with values of 60 and 0.04 respectively.

##### a) Element Densities



##### b) Spatial Gradient (x direction)



##### c) Spatial Gradient (y direction)

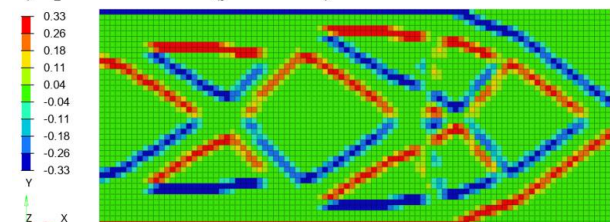


Fig. 2 Spatial gradient calculation in the  $x$  and  $y$  directions for a 2D structured mesh.

#### 3.2 Unstructured 2D mesh

The interface detection approach was applied to the unstructured mesh in Fig. 4a that contains both quadrilateral and triangular elements that are not aligned in the global coordinate system. As noted earlier, some methods of interface detection that rely on a perfectly structured quadrilateral mesh would not be able to calculate the interfaces of this model. The element densities in Fig. 4b were taken from a unconverged optimization result to test the interface detection performance when many intermediate density elements are present. The final interface values are shown in Fig. 4e.

In this example, it is difficult to assign interface values to the group of intermediate density elements at the center of the model. The proposed algorithm detected interfaces at the bounds of this area (where the geometry transitions from intermediate elements to void elements) but did not detect interfaces for some emerging features (where the geometry transitions from solid elements to intermediate density elements). This is due to the thinning calculation,

## Brief Note

which reduces the interface values in all the intermediate density elements. Taking the interface of the penalized element density used in the interpolation of element stiffness would ignore the intermediate density elements and may provide a more meaningful interface calculation. Heaviside projection parameters of  $\beta = 25$  and  $\eta = 0.1$  were used for this problem. Like the thinning step, slight

modifications to this step (e.g. different projection parameters) may provide better results for the intermediate density elements in this problem. When implementing this interface method into topology optimization, progressively increasing the thresholding parameters could be explored to improve boundary detection performance at all stages in the optimization.

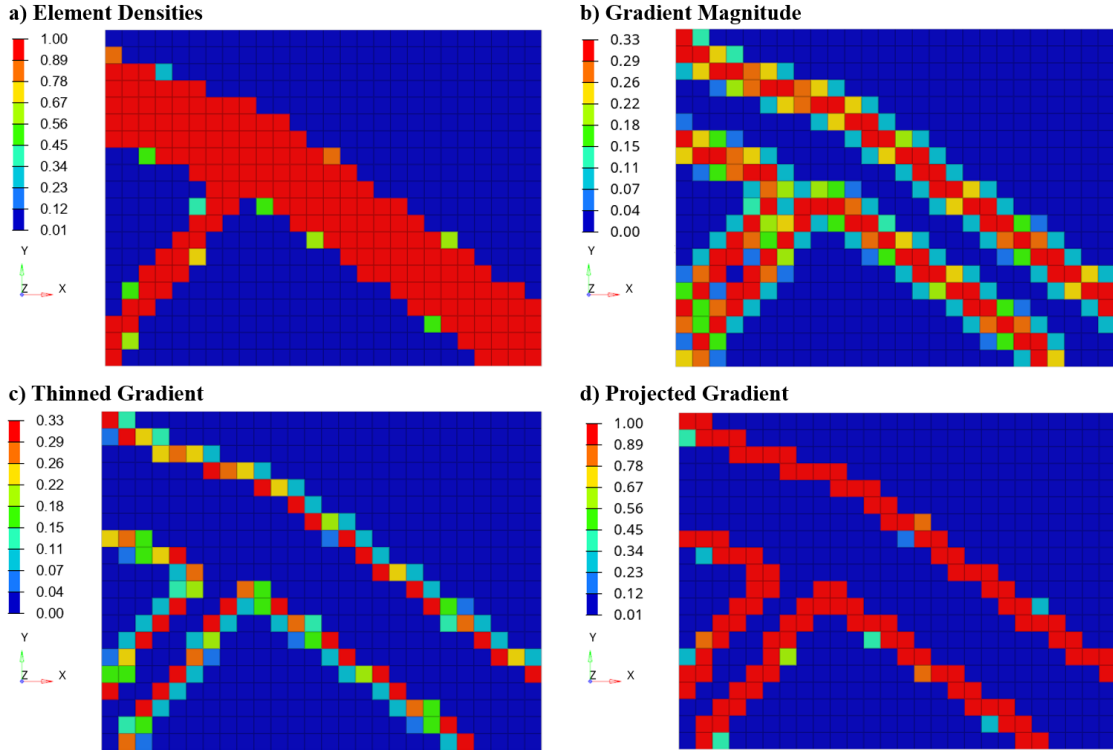


Fig. 3 Interface detection of a 2D structured mesh for a subsection of the example shown in Fig. 2

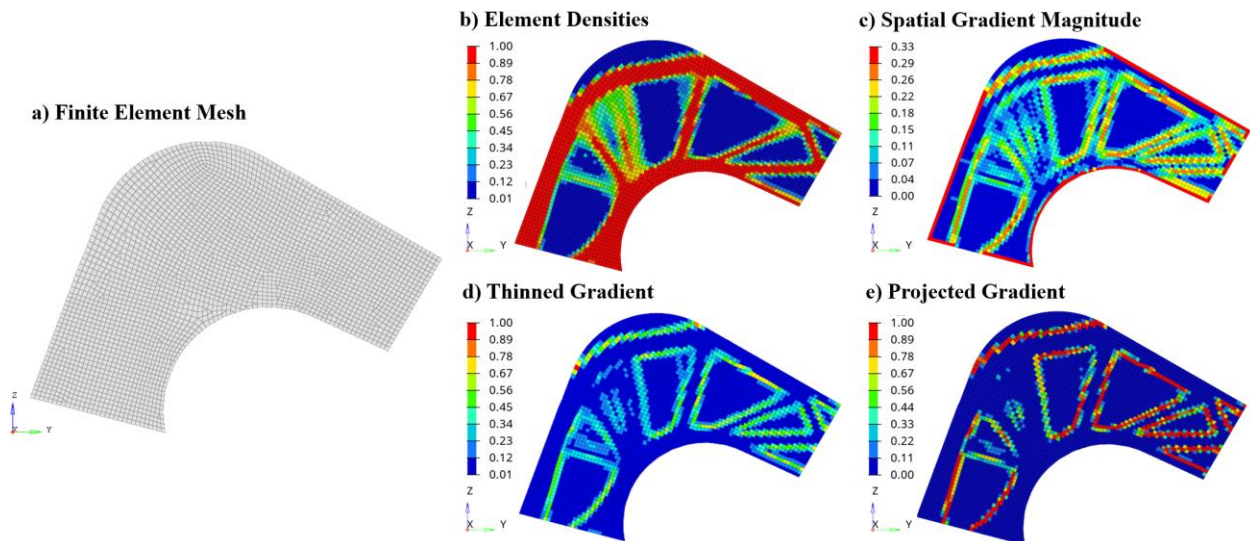


Fig. 4 Interface detection for a 2D unstructured mesh with intermediate density elements.

## Brief Note

### 3.3 Unstructured 3D mesh

The mesh displayed in Fig. 5a contains unstructured tetrahedral elements in a 3D geometry. It can be difficult to evaluate interfaces for this mesh as it contains coarse interior elements, shown in the cross-section of Fig. 5a, which can cause jagged boundaries of the part seen in the element densities in Fig. 5b. Heaviside parameters of  $\beta = 60$  and  $\eta = 0.04$  were used in this example as the elements densities are nearly discrete.

The projected gradient field plotted in Fig. 5c demonstrates that the proposed method accurately calculates interfaces in a complex 3D geometry. The interface field contains some intermediate density elements because of the jagged nature of the element boundaries. Averaged iso-surface plots visually show the 3D geometry and its interface, indicating that the projected gradient field produces a thin layer of elements surrounding the geometry of the part.

## 4 Conclusions

This note presents a detailed methodology for spatial gradient calculation and interface detection suitable for unstructured 2D and 3D meshes. The methodology is

easy to implement in custom topology optimization code that interfaces with black-box finite element solvers. Validation on three numerical problems demonstrates strong performance on topology optimization density fields with unstructured meshes, intermediate density elements, and 3D geometry.

Future work includes the derivation of sensitivity calculations to further aid in the implementation of this methodology. Integration of this spatial gradient and interface calculation technique into topology optimization for different applications is required to fully validate the performance of the methodology.

## 5 Replication of results

A pseudo code is included in Appendix A to assist in replicating the results presented in this note. The code is implemented in 3D and necessary input parameters are specified in the associated numerical examples.

## Compliance with ethical standards

**Conflict of interest** The authors declare that they have no conflict of interest.

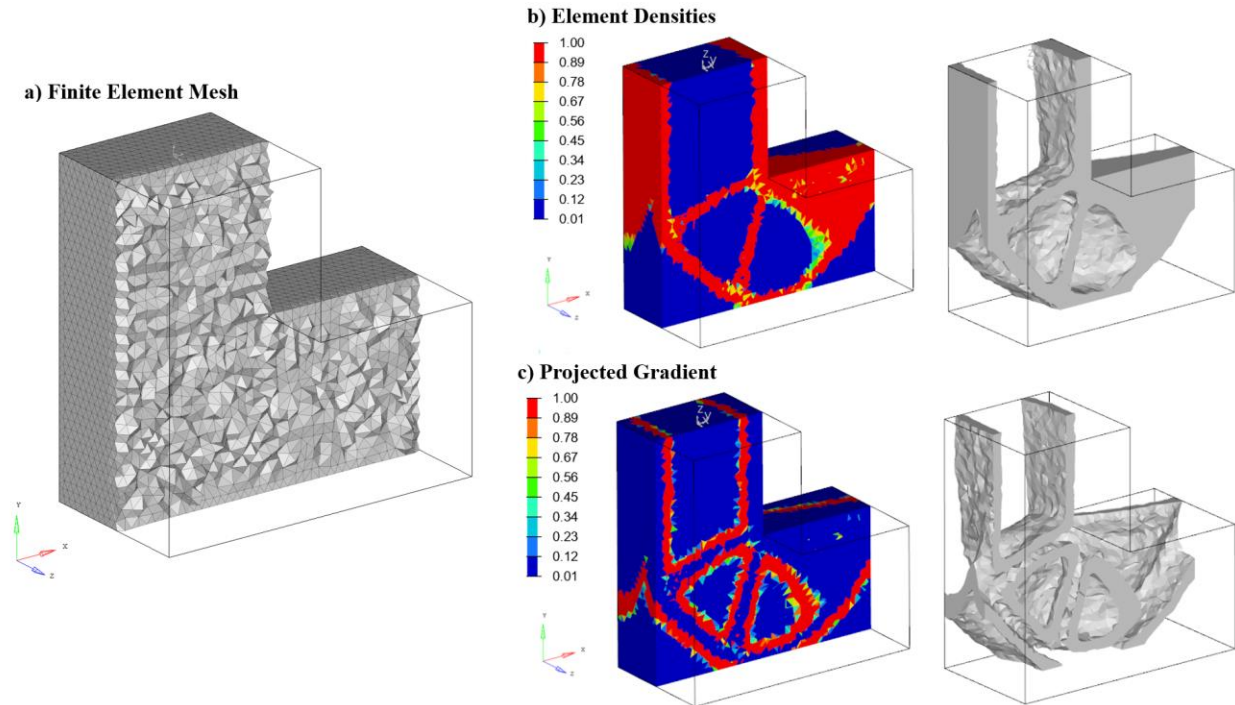


Fig. 5 Interface detection for a 3D unstructured mesh with a section cut applied through the geometry. Iso-surface plots are included to help visualize the 3D geometry

## Brief Note

### Appendix A. Pseudo code

```
subroutine INTERF_DET (NUM_ELEMS, RADIUS, MAX_NUM_ADJ_ELEMS, BETA, ETA)

    integer, intent(in) :: NUM_ELEMS, MAX_NUM_ADJ_ELEMS
    real, intent(in) :: RADIUS, BETA, ETA

    ! Define Variables
    integer :: i,j
    real :: rho(NUM_ELEMS), elemcenter(NUM_ELEMS,3), volume(NUM_ELEMS)
    real :: AdjIDs(NUM_ELEMS,MAX_NUM_ADJ_ELEMS)
    real :: hXSum(3), hSum, vector(3), distance, cosine(3)
    real :: grad(NUM_ELEMS,3),gradmag(NUM_ELEMS), proj_grad(NUM_ELEMS), thin_grad(NUM_ELEMS)

    ! Retrieve Design Variable Values
    call problem%getDVValues(rho)

    ! Retrieve Coordinates of Element Centers
    call problem%getElemCenters(elemcenter)

    ! Retrieve Element Volumes
    call problem%getElemVolumes(volume)

    ! Retrieve Element IDs of Adjacent Elements
    call problem%getAdjElemIDs(RADIUS,AdjIDs)

    ! Calculate Gradient
    do i=1,NUM_ELEMS

        hXSum = 0
        hSum = 0

        ! Calculate Summation Terms for Adjacent Elements
        do j=1,MAX_NUM_ADJ_ELEMS

            vector = elemcenter(AdjIDs(i,j),:) - elemcenter(i,:)
            distance = sqrt(vector(1)**2 + vector(2)**2 + vector(3)**2)
            cosine = vector / distance
            h = max(0.0 , RADIUS - distance)
            hXSum = hXSum + h * volume(AdjIDs(i,j)) * rho(AdjIDs(i,j)) * cosine
            hSum = hSum + h * volume(AdjIDs(i,j))

        end do

        ! Finish Gradient Calculation
        grad(i,:) = hXSum / hSum

        ! Calculate Gradient Magnitude
        gradmag(i) = sqrt(grad(i,1)**2 + grad(i,2)**2 + grad(i,3)**2)

        ! Thin and Project Gradient
        thin_grad(i) = (1 - rho(i)) * gradmag(i)
        proj_grad(i) = 1 / (1 + exp(-2 * BETA * (thin_grad(i) - ETA)))

    end do

end subroutine
```

## Brief Note

### References

- Altair Engineering Inc. (2019) Altair OptiStruct 2019 User Guide.
- Beckers M (1999) Topology optimization using a dual method with discrete variables. *Struct Optim* 17(1):14-24.  
<https://doi.org/10.1007/BF01197709>
- Clausen A, Aage N, Sigmund O (2015) Topology optimization of coated structures and material interface problems. *Comput Meth Appl Mech Eng* 290:524-541.  
<https://doi.org/10.1016/j.cma.2015.02.011>
- Costa Jr JCA, Alves MK (2003) Layout optimization with h-adaptivity of structures. *Int J Numer Methods Eng* 58(1):83-102.  
<https://doi.org/10.1002/nme.759>
- Florea V, Pamwar M, Sangha B, Kim IY (2020) Simultaneous single-loop multimaterial and multijoint topology optimization. *Int J Numer Methods Eng* 121(7):1558-1594.  
<https://doi.org/10.1002/nme.6279>
- Nana A, Cuilliere JC, Francois V (2016) Towards adaptive topology optimization. *Adv Eng Softw* 100:290-307.  
<https://doi.org/10.1016/j.advengsoft.2016.08.005>
- Qian XP (2017) Undercut and overhang angle control in topology optimization: A density gradient based integral approach. *Int J Numer Methods Eng* 111(3):247-272.  
<https://doi.org/10.1002/nme.5461>
- Ryan L, Kim IY (2019) A multiobjective topology optimization approach for cost and time minimization in additive manufacturing. *Int J Numer Methods Eng* 118(7):371-394.  
<https://doi.org/10.1002/nme.6017>
- Sabiston G, Kim IY (2019) 3D topology optimization for cost and time minimization in additive manufacturing. *Struct Multidiscip Optim* 61:731-748. <https://doi.org/10.1007/s00158-019-02392-7>
- Sigmund O (2007) Morphology-based black and white filters for topology optimization. *Struct Multidiscip Optim* 33(4-5):401-424. <https://doi.org/10.1007/s00158-006-0087-x>
- Stainko R (2006) An adaptive multilevel approach to the minimal compliance problem in topology optimization. *Commun Numer Meth Engng* 22(2):109-118. <https://doi.org/10.1002/cnm.800>
- Stolpe M, Svanberg K (2001) An alternative interpolation scheme for minimum compliance topology optimization. *Struct Multidiscip Optim* 22(2):116-124. <https://doi.org/10.1007/s001580100129>
- Woischwill C, Kim IY (2018) Multimaterial multijoint topology optimization. *Int J Numer Methods Eng* 115(13):1552-1579.  
<https://doi.org/10.1002/nme.5908>
- Yang KK, Fernandez E, Niu C, Duysinx P, Zhu JH, Zhang WH (2019) Note on spatial gradient operators and gradient-based minimum length constraints in SIMP topology optimization. *Struct Multidiscip Optim* 60(1):393-400.  
<https://doi.org/10.1007/s00158-019-02269-9>
- Zhou M, Shyy YK, Thomas HL (2001) Checkerboard and minimum member size control in topology optimization. *Struct Multidiscip Optim* 21(2):152-158. <https://doi.org/10.1007/s001580050179>